Conf-8410142--76

EVALUATION OF METHODS FOR LEAK DETECTION IN REACTOR PRIMARY SYSTEMS AND NDE OF CAST STAINLESS STEEL*

CONF-8410142--76

TI85 005056

D. S. Kupperman and T. N. Claytor

Materials Science and Technology Division
Argonne National Laboratory
Argonne, Illinois 60439

and

D. W. Prine and T. A. Mathieson

Chamberlain Mfg. Corporation
GARD Division
Niles, Illinois 60648

September 1984

*Work supported by the U.S. Nuclear Regulatory Commission, Office of Nuclear Regulatory Research.

To be presented at the 12th Water Reactor Safety Research Information Meeting, October 22-26, 1984, sponsored by the U.S. Nuclear Regulatory Commission, Washington, DC.

EVALUATION OF METHODS FOR LEAK DETECTION IN REACTOR PRIMARY SYSTEMS AND NDE OF CAST STAINLESS STEEL

D. S. Kupperman and T. N. Claytor
Materials Science and Technology Division
Argonne National Laboratory
Argonne, Illinois 60439

and

D. W. Prine and T. A. Mathieson
Chamberlain Mfg. Corporation
GARD Division
Niles, Illinois 60648

ABSTRACT

No currently available, single leak-detection method combines optimal leakage detection sensitivity, leak-locating ability, and leakage measurement accuracy. Technology is available to improve leak detection capability at specific sites by use of acoustic monitoring. However, current acoustic monitoring techniques provide no source discrimination (e.g., to distinguish between leaks from pipe cracks and valves) and no leak-rate information (a small leak may saturate the system). Leak detection techniques need further improvement in the following areas: (1) identifying leak sources through location information and leak characterization, to eliminate false calls; (2) quantifying and monitoring leak rates; and (3) minimizing the number of installed transducers in a "complete" system through increased sensitivity.

Six cracks, including two field-induced IGSCC specimens and two thermal-fatigue cracks, have been installed in a laboratory acoustic leak detection facility. The IGSCC specimens produce stronger acoustic signals than the thermal-fatigue cracks at equivalent leak rates. Despite significant differences in crack geometry, the acoustic signals from the two IGSCC specimens, tested at the same leak rate, are virtually identical in the frequency range from 200 to 400 kHz. Thus, the quantitative correlations between the acoustic signals and leak rate in the 300-400 kHz band are very similar for the two IGSCC specimens. Also, acoustic background data have been acquired during a hot functional test at the Watts Bar PWR. With these data, it is now possible to estimate the sensitivity of acoustic leak detection techniques. In addition, cross-correlation techniques have been successfully used in the laboratory to locate the source of an electronically simulated leak signal.

The adequacy of current inspection techniques for cast stainless steel (CSS) piping has not been demonstrated. For the near term, improvements that may increase the reliability of ultrasonic inspection include (1) the development of methods to establish the microstructure of the material (to help optimize the

*Work supported by the U.S. Nuclear Regulatory Commission, Office of Nuclear Regulatory Research.

inspection technique), (2) calibration standards that are more representative of the material to be inspected, and (3) the use of cracked CSS samples for training purposes. For the long term, it will be necessary to establish (1) the variability of the microstructure of CSS, (2) the effect of microstructure on inspection reliability, and (3) the degree of improvement possible with techniques and equipment designed specifically for CSS, e.g., focused transducers and lower frequencies than those used conventionally.

I. LEAK DETECTION IN REACTOR PRIMARY SYSTEMS

A. Background

No currently availabile single leak-detection method combines optimal leakage detection sensitivity, leak-locating ability, and leakage measurement accuracy. For example, while quantitative leakage determination is possible with condensate flow monitors, sump monitors, and primary coolant inventory balance, these methods are not adequate for locating leaks and are not necessarily sensitive enough to meet regulatory guide goals. The technology is available to improve leak detection capability at specified sites by use of acoustic monitoring or moisture-sensitive tape. However, current acoustic monitoring techniques provide no source discrimination (e.g., to distinguish between leaks from pipe cracks and valves) and no leak-rate information (a small leak may saturate the system). Moisture-sensitive tape provides neither quantitative leak-rate information nor specific location information other than the location of the tape; moreover, its usefulness with "soft" insulation needs to be demonstrated. Hence, leak detection techniques need further improvement in the following areas: (1) identifying leak sources through location information and leak characterization, to eliminate false calls; (2) quantifying and monitoring leak rates; and (3) minimizing the number of installed transducers in a "complete" system through increased sensitivity.

B. Objectives

The objectives of the leak detection program are to (a) develop a facility for the quantitative evaluation of acoustic leak detection (ALD) systems; (b) assess the effectiveness and reliability of ALD techniques; (c) evaluate a prototype ALD system; (d) establish the sensitivity, reliability, and decision-making capability of a prototype system through laboratory testing; and (e) assess the effectiveness of field-implementable ALD systems. The program will establish whether meaningful quantitative data on leak rates and location can be obtained from acoustic signatures of leaks due to IGSCC and fatigue cracks in low- and high-pressure lines, and whether these can be distinguished from other types of leaks. It will also establish calibration procedures for acoustic data acquisition and show whether advanced signal processing can enhance the adequacy of ALD schemes.

C. Review of Current Practice

Regulatory Guide 1.45 recommends the use of at least three different detection methods in reactors to detect leakage. Monitoring of both sump-flow and airborne-particulate radioactivity is mandatory. A third method can involve either monitoring of condensate flow rate from air coolers or monitoring of airborne gaseous radioactivity. Although the current methods used for leak detection reflect the state of the art, other techniques may be developed and used. Regulatory Guide 1.45 also recommends that leak rates from identified and unidentified sources be monitored separately to an accuracy of 1 gal/min,* and that indicators and alarms for leak detection be provided in the main control room.

Since the recommendations of Regulatory Guide 1.45 are not mandatory, the technical specifications for 74 operating plants including PWRs have been reviewed by the present authors to determine the types of leak detection methods employed, the range of limiting conditions for operation, and the surveillance requirements for the leak detection systems.

All plants use at least one of the two systems specified by Regulatory Guide 1.45: All but eight use sump monitoring, and all but three use particulate monitoring. Monitoring of condensate flow rate from drywell air coolers and monitoring of atmospheric gaseous radioactivity are also used in many plants.

The allowed limits on unidentified coolant leakage are shown in Fig. 1 (upper panel). The limit for all PWRS is 1 gal/min, whereas the limit for most BWRs is 5 gal/min. The limits on total leakage (Fig. 1, lower panel) are generally 10 gal/min for PWRs and 25 gal/min for BWRs. (Regulatory Guide 1.45 does not specify leakage limits, but does suggest that the leakage detection system should be able to detect a 1-gal/min leak in 1 h.) In some cases, limits on rates of increase in leakage are also stated in the plant technical specifications. Two BWRs have a limit of 0.1 gal/min/h; four have a limit of 0.5 gal/min/h.

Surveillance periods for BWRs and PWRs are indicated in Fig. 2 (upper panel). Leakage is checked every 12 h in most PWRs, and every 4 or 24 h in most BWRs. One BWR specifies that a continuous monitor with control room alarm shall be operational. The intervals between successive system calibrations and checks are indicated in Fig. 2 (lower panel). For BWRs, calibration is generally performed at 18-month intervals; functional tests are performed every month.

Generally speaking, reactors rely on sump pump monitoring to establish the presence of leaks. Other methods appear to be less reliable or less convenient. In most reactors the surveillance periods are too long to detect a 1-gal/min leak in 1 h, as suggested by Regulatory Guide 1.45, but it appears that this sensitivity could be achieved if monitoring procedures were modified. None of the systems provides any information on leak location, and leaks must be located by visual examination after shutdown. Since cracks may close when the reactor is shut down, reducing flow rates considerably, it would be desirable to be able to locate cracks during plant operation.

---

*Conversion factor: 1 gal/min = 3800 cm^3/min.

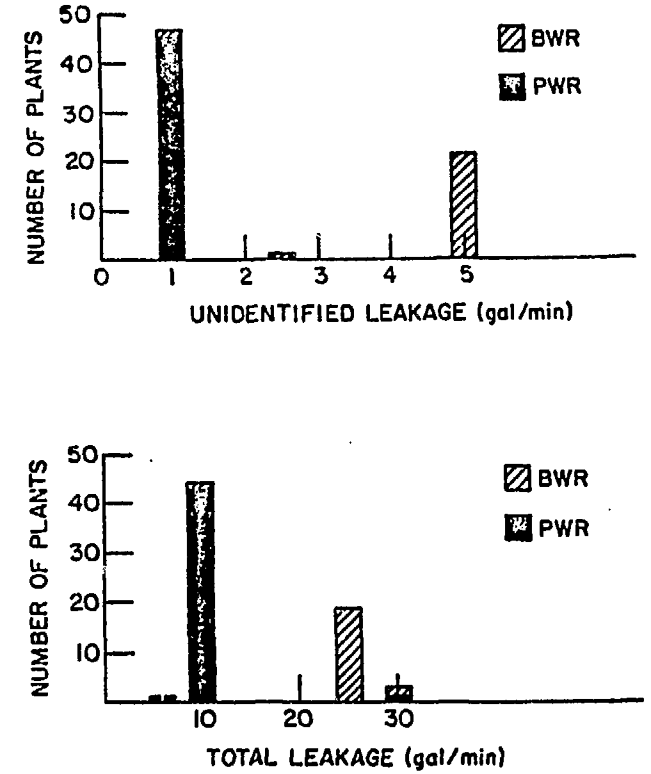

Fig. 1. Amounts of Unidentified and Total Coolant Leakage Allowed at BWRs and PWRs. Conversion factor: 1 gal/min = 3800 cm^3/min.

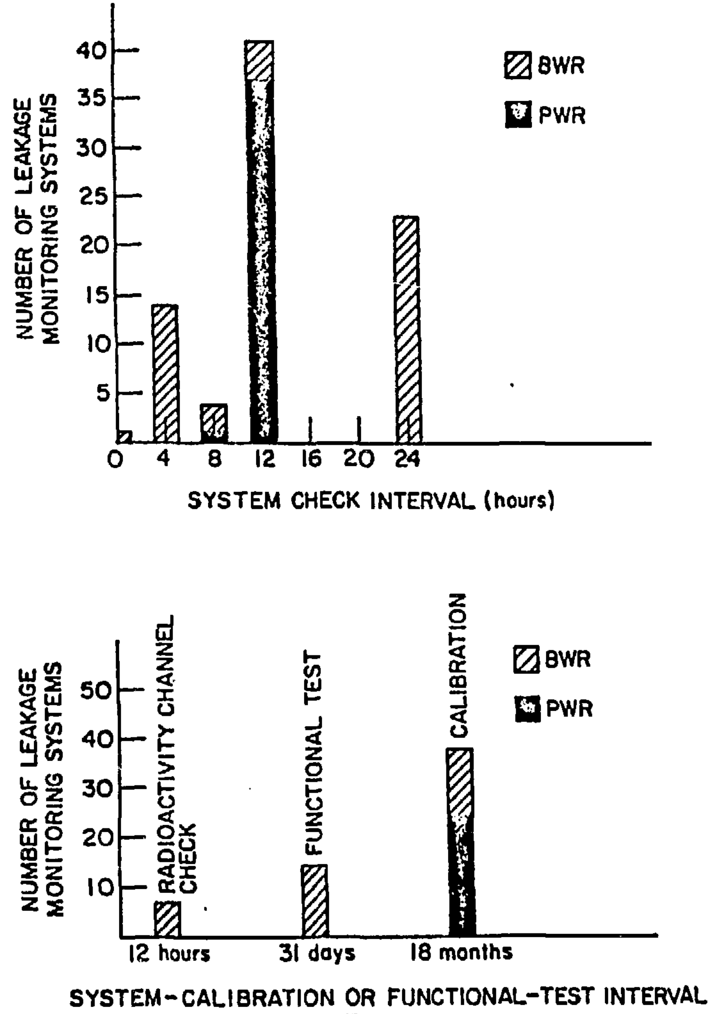

Fig. 2. Surveillance Periods (Top) and Test Calibration Intervals (Bottom) for BWRs and PWRs.

The estimated sensitivity of leakage monitoring is occasionally addressed in the technical specifications. For example, one specification indicates that air particulate monitoring can, in principle, detect a 0.013-gal/min leak in 20 min, that the sensitivity of gas radioactivity monitoring is 2-10 gal/min, and that the sensitivity of condensate flow monitoring is 0.5-10 gal/min. Continuous sump pump monitoring appears capable of detecting a 1-gal/min leak in 10-60 min.

The impact of Reactor Coolant Pressure Boundary leakage detection systems on safety was evaluated for eight reactors as part of the Integrated Plant Safety Assessment-Systematic Evaluation Program (SEP) and described in eight SEP reports (NUREG-0820 through -0827). In four of the eight reactors evaluated, a 1-gal/min leak could not be detected within 1 h; and four of the eight reactors did not have three leakage monitoring systems, contrary to the suggestions in Regulatory Guide 1.45. The fracture mechanics and leak rate calculations in the SEP reports are consistent with other studies which indicate that (1) current leak detection systems will detect through-wall cracks 10-25 cm (4-10 in.) long in 12- to 28-in. piping within one day, and (2) current leakage limits will necessitate plant action after such a detection event. Since these cracks are much smaller than those required to produce failure in tough reactor piping, improved leak detection systems may offer little safety benefit for this particular class of flaws when crack growth occurs by a relatively slow mechanism. However, the SEP reports state that local leak detection systems may be necessary for some postulated break locations where separation and/or restraint is not a practical way to mitigate the effects of a high-energy pipe break.

Although current leak detection systems are adequate to ensure a leak-before-break scenario in the great majority of situations, the possibility that large cracks may produce only low leak rates must also be considered. This could arise because of corrosion plugging or fouling of relatively slowly growing cracks or the relatively uniform growth of a long crack before penetration. In such cases the time required for a small leak to become a significant leak or rupture could be short, depending on crack geometry, pipe loading, and transient loading (a seismic or water hammer event). Furthermore, with existing techniques such as sump pump monitoring, no information on leak location is available.

The shortcomings in existing leak detection systems are not simply a matter of conjecture. The Duane-Arnold safe-end cracking incidents and Indian Point Unit 2 fan cooler leakage indicate that the sensitivity and reliability of current leak detection systems are clearly inadequate in some cases. In the Duane Arnold case, the plant was shut down on the basis of the operator's judgment when a leak rate of 3 gal/min was detected; however, this leakage rate is below the required shutdown limit for almost all BWRs (see Fig. 1). Examination of the leaking safe-end showed that cracking had occurred essentially completely around the circumference. The crack was throughwall over about 20% of the circumference and 50-75% throughwall in the non-leaking area.

Simply tightening the current leakage limits is not an adequate solution to these shortcomings, since this might produce an unacceptably high number of spurious shutdowns owing to the inability of current leak detection systems to identify leak sources.

One other safety-related aspect of improved leak detection systems concerns radiation exposure of plant personnel. Improved systems with leak location capability could reduce the exposure of personnel inside the containment and could present an attractive alternative to augmented ISI. Improved leak detection is consistent with the defense-in-depth philosophy of the NRC and would lead to earlier detection of system degradation.

D. Technical Progress

1. Comparison of Acoustic Leak Data from Different Crack Types

Two IGSCC specimens, two thermal fatigue cracks (TFCs), and one mechanical fatigue crack (FC) have been installed in the ALD facility at ANL. The crack widths and lengths at the pipe outer surface are indicated in Table 1. Figure 3 shows acoustic leak data acquired from these five cracks. These data are normalized to a 375-kHz acoustic emission (AET-375) transducer on a waveguide with a water temperature of 260°C (500°F) and pressure of 7.7 MPa (1100 psi). The largest correction is for the mechanical fatigue crack FC #1. Corrections for the other data are less than 6 dB. Transducer signals indicated in Fig. 3 are for a 300-400 kHz bandwidth and represent the signal after electronic noise levels are subtracted. The acoustic signals from the fatigue cracks vary approximately as $(\text{leak rate})^{0.7}$, whereas the signals from the IGSCC vary approximately as $(\text{leak rate})^{0.37}$. Frequency analysis also indicates less dependence of acoustic signal on frequency for the IGSCC specimens than for the fatigue cracks. An analysis of the frequency spectrum may provide information on the source of acoustic leak signals. The excellent matching of acoustic leak data in the 300-400 kHz range for the two IGSCC specimens, despite their different geometries, suggests that it may be possible to derive leak rate information from the amplitude of the acoustic leak signal in this frequency range.

Table 1. Outer-Surface Lengths and Widths of Cracks Used in ALD Studies

Crack	Length, cm	Width, μm
IGSCC #1	0.23	90
IGSCC #2	1.10	60–80
TFC #1	2.64	75–100
TFC #2	1.24	40–100
FC #1	0.52	150–200

Detection of a leak requires that $S_e = S_1 - T_1 - N_1 + PG > 0$, where S_e = signal excess at detector output, S_1 = source level (affected by waveguide geometry, insulation, and circumferential position), T_1 = transmission loss down pipe, N_1 = background noise level, and PG = system gain (all in dB). The acquisition of acoustic leak data, background noise estimates (from Hatch and Watts Bar), and attenuation data allows a rough estimation of the sensitivity of an ALD system under field conditions. Figure 4 shows predicted signal-to-noise ratios (in dB) vs distance along a 10-in. Schedule 80 pipe for three leak rates and three levels of estimated acoustic background noise.

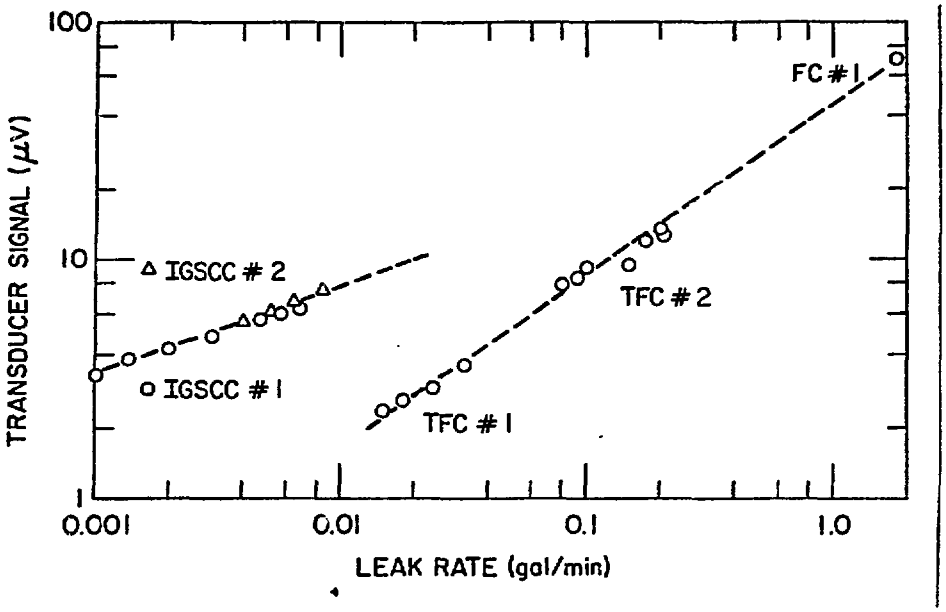

Fig. 3. Acoustic Leak Data from the Cracks Listed in Table 1. Data are normalized as described in the text. Signal amplitudes are for a 300-400 kHz bandwidth after electronic background noise is subtracted.

The highest level is estimated from the maximum acoustic level obtained during the Watts Bar hot functional test when the reactor was at operating temperature and pressure. The lowest level is obtained from an indirect estimate of background noise from Hatch and the assumptions that the reactor acoustic background level will vary by a factor of 10 in the plant and that the measurement at Watts Bar was an upper-limit value. The striped area suggests possible enhancement of the acoustic signal for a 0.1-gal/min leak rate in a situation where the leak plume strikes the reflective insulation. Results of laboratory experiments suggest that for leak rates greater than 0.02 gal/min but less than 0.2 gal/min, signals could be enhanced significantly, given the correct circumstances. The following equation has been used to generate the curves of Fig. 4:

$$S = 20 \log_{10} \left(\frac{70R^{0.32}}{B}\right) - \begin{Bmatrix} 4.5D \text{ for } D < 3 \text{ m} \\ 5.6 + 1.7D \text{ for } D \geq 3 \text{ m} \end{Bmatrix} + \left\{ 6 \text{ if } 0.01 < R \leq 0.1 \right\} , \quad (1)$$

where S is the signal-to-noise ratio in dB, R is the leak rate in gal/min, B is the acoustic background level in μV (4, 20, or 40), and D is the distance from the leak in meters. Equation (1) assumes a signal loss of 4.5 dB for the first 2 m, followed by a further loss of 1.7 dB/m. The acoustic signal is assumed to vary as (leak rate)$^{0.32}$. A 6-dB signal enhancement is added to the 0.1-gal/min curve to indicate how the presence of reflective insulation could improve the signal-to-noise ratio. For low acoustic background levels, a 1-gal/min leak would be detected at a distance of 11 m. With a high background level, this leak would be detected only at a distance of 1 m.

Acoustic leak data have also been obtained from a small (13-mm-diam) valve with a stem leak. An AET-375 transducer, on a waveguide attached directly to the valve body, was employed to acquire data from a 0.01-gal/min, 270°C (520°F) leak. The signal obtained was 35 dB above the electronic background level.

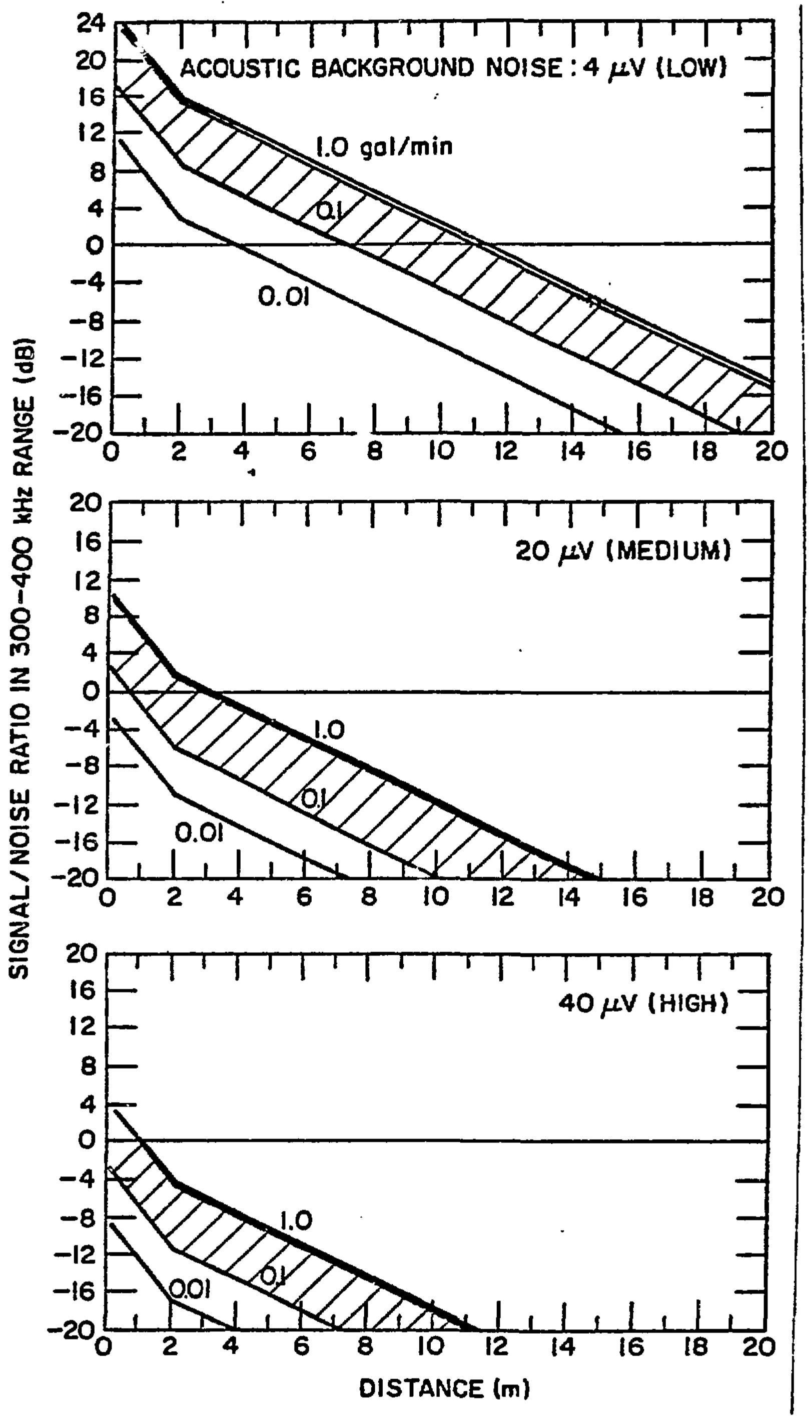

Fig. 4. Predicted Acoustic Signal-to-Noise Ratios vs Distance along a 10-in. Schedule 80 Pipe for Three Leak Rates and Three Levels of Estimated Acoustic Background Noise. The striped areas indicate possible enhancement of the signal for the 0.1 gal/min leak because of the presence of reflective insulation.

This is considerably higher than signals obtained from IGSCC specimens with similar leak rates. Further analysis of valve leak signals is in progress to establish whether valve leaks can be distinguished from crack leaks.

Studies have also been carried out to establish the effect of "Nu-Kon" fiberglass insulation on the generation and attenuation of acoustic leak signals. Analysis of the results suggests that this "soft" insulation has very little effect on the generation or propagation of acoustic leak signals.

2. Spectral Analysis of Acoustic Background Noise

The background noise data acquired during a hot functional test of the TVA's Watts Bar Reactor in Tennessee has been evaluated with regard to spectral content. In this test, an AET-375 transducer was mounted on the accumulator safety injection pipe on the cold leg of loop 2. A 25.4-cm-long waveguide was employed. The responses of this transducer to the acoustic background noise and an acoustic leak signal were compared. The acoustic leak signal response of the very-broadband NBS-designed IQI-501 transducer served as a reference. The frequency spectrum of the acoustic background noise showed a slight (<2 dB) drop in amplitude in the 250-kHz region when compared with a monotonically decreasing background noise curve. This adds some further support to the belief that the optimum frequency window for acoustic leak monitoring is 200-400 kHz.

3. Cross-Correlation Analysis

Results of recent experiments on the application of cross-correlation analysis for acoustic leak location have been encouraging. Electronically generated white noise, simulating acoustic waves from leaks, was injected into the 10-in. piping of the ALD facility. Strong correlations were obtained in the 200-400 kHz range with "matched" AET-375 transducers on waveguides separated by a distance of about 1 m. These tests were carried out on a part of the pipe run that was filled with water and included an elbow with two welds. Figure 5 shows the cross-correlation function for a simulated leak signal and waveguides separated by 1.4 m. The acoustic source consisted of a white noise generator driving a PZT-5 pressure-bonded crystal on a rod threaded into the pipe between the waveguides, 0.1 m from one waveguide. The peak is slightly off center, as expected. The radio frequency signals were envelope detected before being analyzed by a Spectral Dynamics 375 signal processor. A wave velocity of 1400 m/s was calculated from the 0.86-ms transit time difference and the 1.2-m difference in waveguide/signal-source separation. This is close to the velocity of longitudinal waves in water (1500 m/s). When the pipe is filled with water, the acoustic leak signal is propagated predominantly through the water. With the pipe drained, the measured velocity is close to the velocity of surface waves in steel, as expected. Correlations for leaks through field-induced cracks were evident, but they were much weaker than for the electronically generated acoustic waves. This may be the result of the complex geometry in the vicinity of the IGSCC (pressure vessel below the crack, heating bands, and extensive welding in the vicinity of the crack).

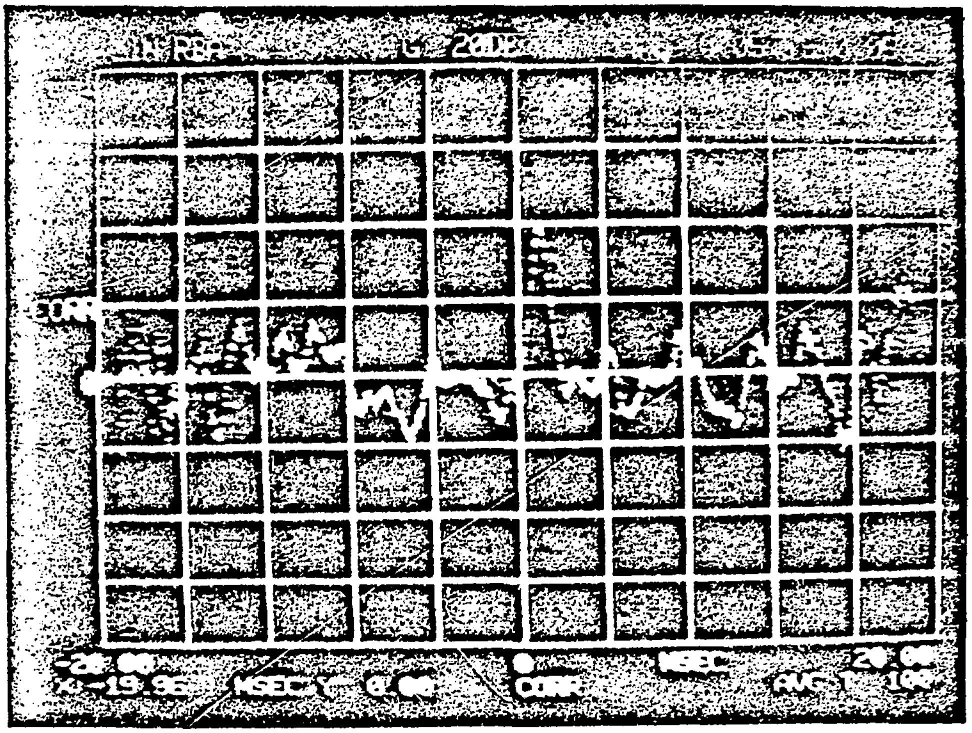

Fig. 5. Cross-Correlation Function for Simulated Leak Signal. The source is located between two AET-375 transducers on waveguides, which are separated by 1.4 m; one waveguide is 0.1 m from the source. The radio frequency signals were envelope detected before being analyzed by a Spectral Dynamics SD 375 signal processor.

4. Calibration Procedures

Three calibration procedures are being considered for checking transducer-waveguide systems after field installation. They are the pencil-lead-breaking method, the gas jet method, and electronic pulsing.

In the lead-breaking technique, the 0.5-mm-dia lead of a Pentel mechanical pencil is extended 5 mm beyond the end of the pencil body and is pressed against the pipe, at an angle of 30° to the pipe, until it breaks. (If this technique is demonstrated to be useful, fixtures will be fabricated to standardize the procedure.) The breaking of the lead was detected by an AET-375 transducer mounted on a waveguide at a distance of 0.2 m from the pipe surface. Excellent reproducibility of the captured acoustic transient signal was evident from a comparison of the digitized and stored transient pulses of four successive breaks. This technique may be useful as a convenient and rapid way to check the ALD system after installation. However, the method would not be applicable to remote in-situ calibration. This could be carried out by the gas jet technique or by electronic pulsing.

In preliminary work on the gas jet technique, a jet of nitrogen gas from the 1.5-mm-dia exit hole of a Swagelok fitting was directed normal to the pipe surface from a distance of 6 mm. An rms signal (50 kHz to 1 MHz) with a magnitude 4 times that of electronic background was detected at a distance of 1 m. The broadband IQI-501 transducer was employed to obtain information on frequency spectra. The acoustic spectrum from the gas jet shows greater frequency dependence than does the spectrum from a leak through an intergranular crack. Relatively more signal at lower frequencies is present in the gas jet spectrum. Furthermore, most of the detected gas-jet acoustic signal is in the form of surface waves; this is not the case for crack leaks. It has also been determined that the acoustic signal is relatively insensitive to the exact height of the gas jet above the surface for heights of about 10 mm. This technique appears to be well suited to remote calibration. Its chief disadvantages are the inconvenience associated with setting up the system and problems associated with the presence of insulation.

The sending of electronic pulses to a calibrating transducer is also under investigation as a technique for remote calibration. In this technique, an electronic signal is used to pulse a transducer (on a waveguide) which then generates an acoustic signal in the pipe. Since a different transducer is used to receive acoustic leak signals, a method would have to be established for distinguishing anomalous behavior of receivers from anomalous behavior of pulsers. The electronic pulsing technique is a relatively simple procedure for continuous in-situ monitoring of an ALD system. The disadvantage is the need for additional transducers on the pipe and possible problems in coupling the waveguides of the transmitting transducers to the pipe.

5. Processing of Acoustic Leak Data

Progress has been made in the evaluation of an ALD system that could be employed in the field. Software accomplishments have included the establishment of a precise test procedure for correlogram computation, the writing of a new correlation subroutine, and the discovery and elimination of "bugs" in the operator interaction routines. The leak detector's internal function generator was enhanced to include exponential enveloping and linear frequency modulation capabilities. With the aid of the latter, functions with characteristic correlogram patterns were generated and used as data sets for testing the IEEE FFT-based correlation routines. Autocorrelograms were computed as expected, but cross-correlograms rarely yielded the expected results. However, FORTRAN programs computing the straightforward time domain solution for the same data set yielded the expected results.

Because time domain computations written in FORTRAN take so long to execute (5 minutes in our test case) and because the time expenditure in analyzing the IEEE correlator insufficiency was felt to be unpredictable at best and prohibitive at worst, a time domain correlation routine callable from a FORTRAN program was written in 68000 assembler language. This routine has been tested and found to give excellent results. It also executes in one-quarter of the time required by the IEEE FFT-based correlator.

A serious bottleneck in the processing of ALD data is in the transfer of the raw data from the transient signal recorders in the CAMAC crate to the host computer system. Currently, the communications link consists of a Kinetic Systems Model 3989 RS-232 crate controller interfaced to our Dual Systems 83/20 computer system through a Dual SIO/DMA Intelligent Four-Port Serial I/O board.

The main problems faced are as follows: (1) The serial I/O board allows direct memory access (DMA) transfer on output only; on input, the host CPU must transfer the data one byte at a time into primary memory. (2) Since the host computer's operating system is a multiuser, multitasking system, we are allotted only small "time slices" in which to accomplish the transfer. Apparently, the duration of one such time slice is not sufficient to allow the transfer of an entire block of data from the transient signal recorders to the host computer.

To overcome these problems, we have decided to use a bit-parallel rather than an RS-232 byte-serial interface. A parallel interface is, with proper handshaking, inherently faster than a serial interface. A brief investigation of the commercially available systems for parallel interfacing of a CAMAC crate controller to an IEEE-696-standard backplane computer showed these to be generally too expensive and too inflexible for our needs. For this reason, we intend to add a parallel port to the existing (serial interface) crate controller. The crate controller PROM firmware will be partially rewritten to support parallel transfers. In addition, we will design an I/O channel controller for the host computer system. This controller will have the ability to drive the host's buses on both output and input operations. Since the controller will have complete control of the host system's resources during CAMAC crate I/O operations, the interference from the host's operating system will be completely avoided. Using the CAMAC block transfer protocol, we will be able to transfer an entire block of data at one time, without concern for operating-system housekeeping activities.

Additional efforts to speed up the data processing are being applied in the area of special-purpose signal processing hardware. As it now stands, the transfer of acoustic leak data from the transient signal recorder to S-100 RAM is the single most time-consuming operation in the entire data reduction process. This situation will change appreciably when we have modified the CAMAC crate controller-to-S-100 bus interface so that data can be transferred in parallel rather than serially; a 50-to-1 improvement in transfer time is expected. At that point, the main cause of delay will become the correlation algorithm itself.

6. Evaluation of Moisture-sensitive Tape

Tests have been carried out to help assess the effectiveness of moisture-sensitive tape for leak detection. Tapes were supplied by Techmark. Figure 6 shows a schematic representation of the facility used for these tests. Leaks are simulated by feeding water through a copper tube to the surface of a 10-in. Schedule 80 pipe. The tapes are located at three positions on the bottom of the pipe, which is tilted approximately 1° as indicated. The pipe is wrapped with either reflective insulation or "soft" insulation (Nu-Kon). The "soft" insulation allows water vapor to penetrate to its outer surface and severely limits the useful range of the tape. Table 2 shows the response time of the tape under various experimental conditions. With Nu-Kon in place and the tape placed directly below the leak (test 10), a 0.05-gal/min leak could be detected in about 12 min. With the tape 2 m away (test 11), the leak could not be detected. However, when the reflective insulation was used (test 7) with the same combination of leak and tape positions as in test 11, the leak was detected in about 10 min. The relative positions of leak and tape on a slightly tilted pipe can have a significant effect on the response

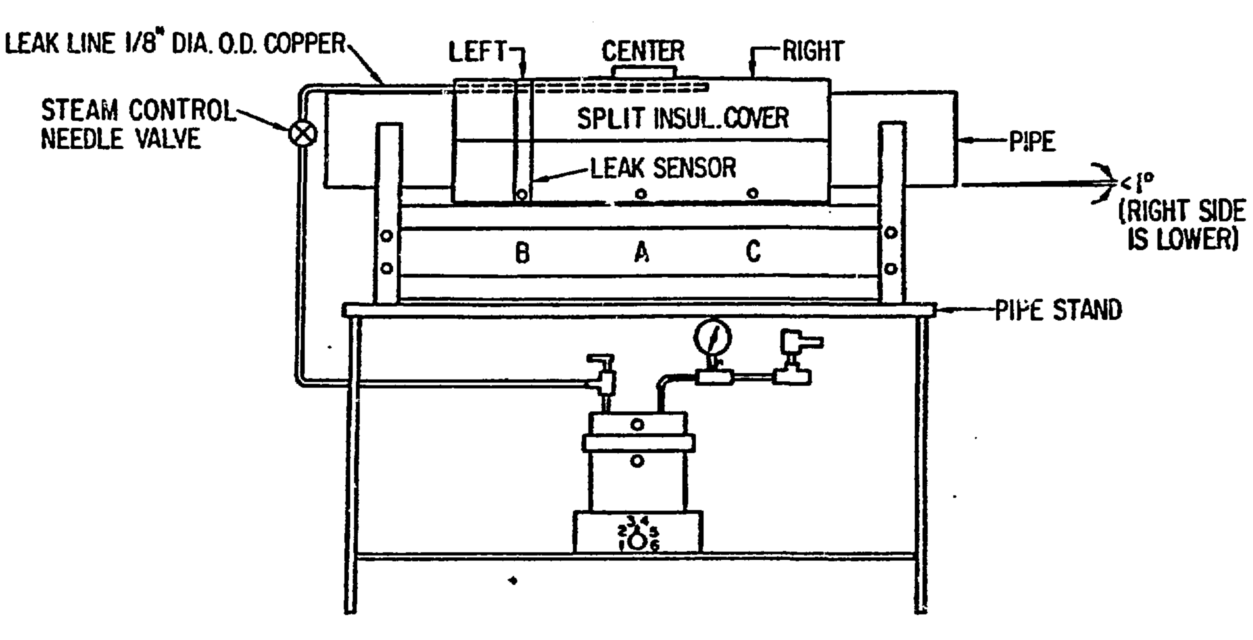

Fig. 6. Schematic Representation of Facility Used to Evaluate Moisture-sensitive Tape. The leak source is placed at one of the indicated positions along the top of the pipe; the leak sensor is placed at one of the three corresponding positions along the bottom. The distance between the center position and the left or right position is about 1 meter.

time, as indicated by the data from tests 1-3. In this case, the tape was able to detect a 0.01-gal/min leak in about 60 min when it was 1 m downstream of the leak, but it did not detect the leak even after 150 min from a location 1 m upstream of the leak. As indicated in tests 5 and 7, however, larger leaks can be detected upstream over these relatively short distances.

The analysis of these results suggests that moisture-sensitive tape may be useful for the detection of leaks in reactors. Under the right conditions, the tapes can detect leaks of the order of 0.01 gal/min. The tapes, however, will be significantly more effective in systems that employ reflective insulation. Despite the sensitive nature of the tapes, they do not provide any quantitative data other than the location at which the system has been triggered. A large leak a long distance from the tape could cause the same response as a small leak at a short distance.

E. Summary

Current leak detection practices in 74 operating nuclear reactors have been reviewed. Although the current leak detection systems are adequate to ensure a leak-before-break scenario in most situations, there is the possibility that large cracks may produce low leakage rates (from corrosion fouling, for example). In such cases, the time required for a small leak to become large could be short. In addition, no leak location information is available with existing systems. Simply tightening current leakage limits may produce an unacceptably large number of unnecessary shutdowns.

Table 2. Response of Moisture-sensitive Tape to Small Leaks

Test	Tape Location[a]	Leak Location[a,b]	Type of Insulation[c]	Flow Rate, gal/min[d]	Water Temperature, °F[d]	Water Pressure, psi[d]	Response Time, min
1	center	center	R	0.01	500	1000	3.8
2	right	center	R	0.01	500	1000	60.2
3	left	center	R	0.01	500	1000	>150.0
4	center	right	R	0.01	500	1000	>270.0
5	center	right	R	0.05	480	770	9.7
6	left	right	R	0.01	500	1000	>270.0
7	left	right	R	0.05	480	770	10.5
8	center	left	R	0.05	500	800	0.3
9	right	left	R	0.05	500	800	0.5
10	left	left	S	0.05	450	900	12.0
11	left	right	S	0.05	500	1000	>65.0

[a]See Fig. 6.

[b]Right end of pipe was lower than left (1° tilt).

[c]R = reflective insulation; S = soft insulation (Nu-Kon).

[d]Conversion factors: 1 gal/min = 3800 cm^2/min; °C = (°F - 32)/1.8; 1 psi = 7 x 10^3 Pa.

Characterization of acoustic leak signals from IGSCC, combined with information on acoustic background noise levels, allows acoustic signal-to-noise ratios to be estimated for a 10-in. Schedule 80 pipe as a function of distance from the leak. Under ideal conditions, leak rates as low as 0.1 gal/min may be detectable at distances on the order of 10 m. Tests with various types of cracks indicate that quantitative correlations between leak rates and acoustic signals in the 300-400 kHz band are possible for IGSCC. Recent cross-correlation results with simulated acoustic leak signals and 375-kHz acoustic-emission sensors on 3-mm-dia waveguides indicate that correlations should be possible.

Preliminary tests have also been carried out at ANL to evaluate a breadboard ALD system that can carry out cross-correlation analyses (including averaging), monitor acoustic leak signals, and provide spectral information.

An evaluation of moisture-sensitive tape suggests that under the right conditions the tapes can detect leaks on the order of 0.01 gal/min when reflective insulation is used. Despite the sensitivity of the tapes, they do not provide quantitative leak data and a large leak at a long distance can result in the same response as a small leak near the tape.

F. Future Efforts

The capability of acoustic techniques to detect, locate, and size leaks will be further studied. A breadboard ALD system will be used to evaluate field-implementable concepts. Leaks larger than those examined thus far will be studied. These will include IGSCC, thermal fatigue, and, in particular, valve leaks. These data will form a more significant basis for estimating the sensitivity and reliability of ALD.

The monitoring of Watts Bar (in collaboration with PNL) will continue. Additional background noise data will be acquired, along with data from any seal leaks appearing during reactor start-up procedures.

II. NDE OF CAST STAINLESS STEEL

A. Background

It is well known that the coarse grain size and elastic anisotropy of cast stainless steel (CSS) make ultrasonic inspection difficult. Although the ASME code requires inspection of cast stainless piping, it has not been possible to demonstrate that current inspection techniques are adequate.

B. Objectives

For the near term, improvements that may increase the reliability of ultrasonic inspection include (a) the development of methods to establish the microstructure of the material (to help optimize the inspection technique), (b) calibration standards that are more representative of the material to be inspected, and (c) the use of cracked CSS samples for training purposes. For the long term, it will be necessary to establish (a) the variability of the microstructure of CSS, (b) the effect of microstructure on inspection reliability, (c) the degree of improvement possible with techniques and equipment designed specifically for CSS, e.g., focused transducers and lower frequencies than those used conventionally, and (d) qualification of requirements for CSS inspections. Recent work carried out at ANL to address some of these points is presented below.

C. Technical Progress

1. Variation of Sound Velocity with Microstructure

When CSS material is isotropic (equiaxed grains), the variation in velocity is small (<2%), whereas for anisotropic material (columnar grains) the variation in velocity can be as large as 100% for shear waves. The magnitude of the velocity of sound may also be used as a measure of the degree of anisotropy and thus as an indicator of microstructure. Relatively low longitudinal velocities indicate a columnar grain structure, whereas high velocities indicate an equiaxed (isotropic) structure. Intermediate values indicate the presence of both microstructures. The validity of this concept has been demonstrated on CSS samples with different microstructures. Figure 7 shows the longitudinal velocities of sound for seven 400 x 180 x 60-mm samples of a 28-in. pipe provided by Battelle PNL and 18 samples of a comparable large-diameter pipe provided by Westinghouse. The Battelle samples were fabricated from a weldment in which material with a well-defined equiaxed grain structure was joined to material with a well-defined columnar grain structure. The Westinghouse samples were also made from a weldment. These specimens, however, were machined flat and have a coarse and poorly defined grain structure. The velocity of sound was measured by standard pulse-echo methods with a 37-mm-dia, 1-MHz transducer. Echo transit times were measured with a Tektronix oscilloscope. In all cases the longitudinal waves propagate in a radial direction through the pipe wall. As shown in Fig. 7, the equiaxed and columnar sides of the Battelle samples can be easily distinguished by measurements of the longitudinal sound velocity. Also, the sample-to-sample variation is relatively small. The Westinghouse samples, however, show large variations in sound velocity from sample to sample as well as within a sample (two measurements were made on each sample). The wide range of the values is indicative of large variations in the microstructure of these samples. This complex microstructure could cause significant, unpredictable distortion of the ultrasonic waves used to interrogate the material and lead to an unreliable result.

During a visit to the Commonwealth Edison Byron Station, sound velocity was measured in a CSS/carbon steel reference block and two CSS elbows (one each on the steam-generator and pump side of the loop 4 crossover).

On the cast portion of the 7.6-mm-thick reference block, the longitudinal sound velocity was measured by the pulse-echo technique at 11 points covering about 0.01 m^2. No significant difficulties were encountered in making these measurements. The average velocity was 6090 m/s, with a variation of about $\pm$1.5% due to the microstructure. The relatively high sound velocity strongly suggests that the calibration block has an equiaxed grain structure, which may be significantly different from the grain structure of the plant piping and elbows. As a check on the accuracy of the measurement, the carbon steel portion of the reference block was also examined. A sound velocity of 5890 m/s was obtained, which is consistent with previous data for this material.

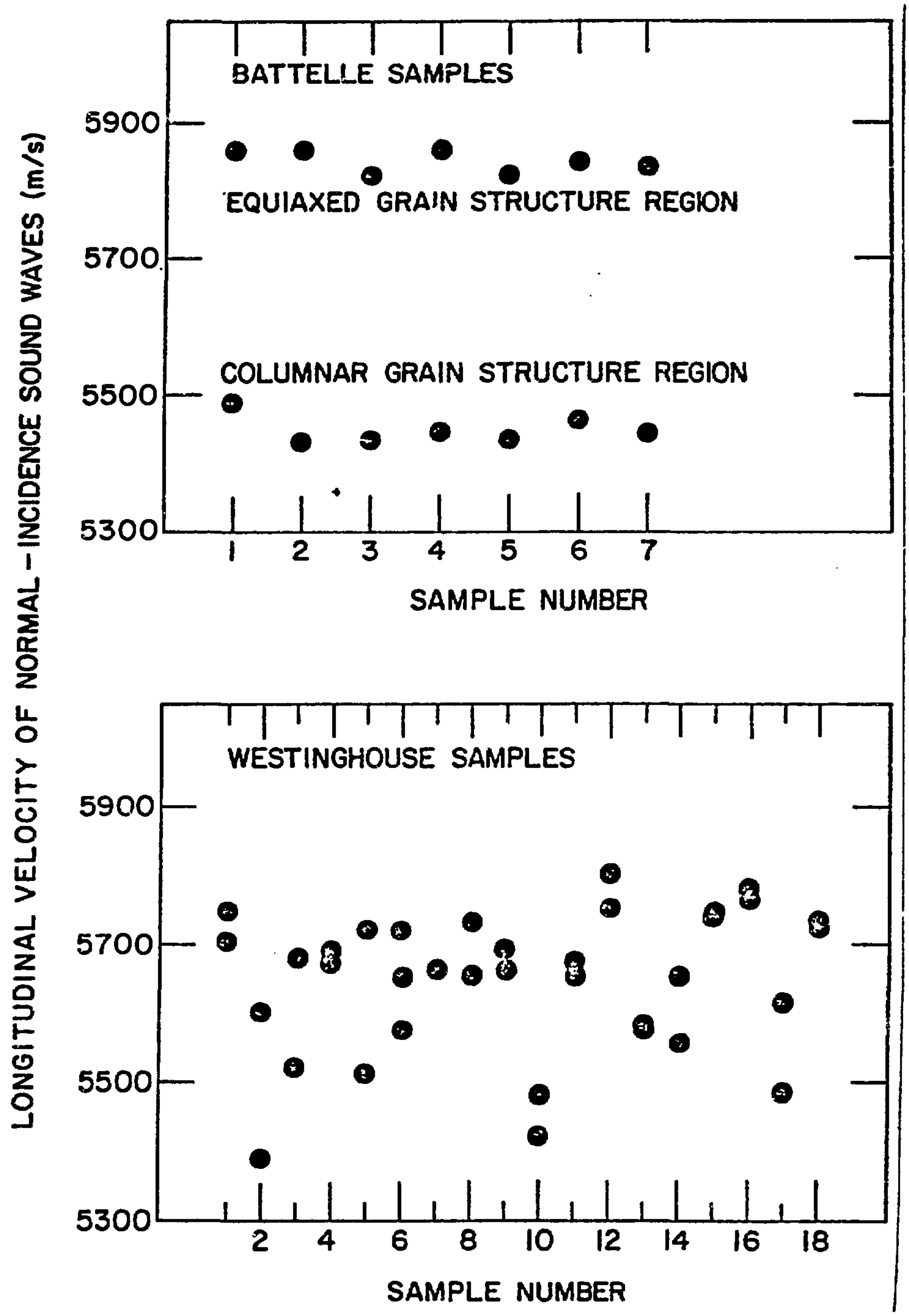

Fig. 7. Variation of Longitudinal Sound Velocity in Large-Diameter CSS Pipe Sections. (Upper panel) samples with both columnar and equiaxed regions; (lower panel) samples with a poorly defined, coarse grain structure. Two measurements were made on each sample. Sample wall thicknesses are nominally 60 mm. 1-MHz, longitudinal waves in a pulse-echo mode were propagated normal to the pipe outer surface.

The surfaces of the CSS elbows were, in most areas, too rough for efficient propagation of ultrasonic waves. Only the smoothly ground areas adjacent to the elbow-to-pipe welds were amenable to pulse-echo examination; ultrasonic backwall echoes could be detected in most, but not all, of these areas. On the pump-side elbow, echoes were detectable at several locations away from the top of the elbow. Since the elbow and pipe appeared to have the same wall thickness, the wall thickness stamped on the pipe section was used as a "best guess" value for the elbow wall thickness. On the basis of this assumption, the sound velocity in the elbow varied from 5200 to 5860 m/s. This suggests that the microstructure of the elbow was quite different from the reference block. The wall thickness of the generator-side elbow could not be estimated because of the elbow geometry, so absolute velocities were not determined; however, it appeared that the velocity varied by about 5%. The velocity of sound in the straight (wrought) section was found to be 5760 m/s, which is consistent with previous measurements on stainless steel.

Attempts were also made to propagate 1-MHz, 45° longitudinal waves in the cast material with two transducers in a pitch-catch mode. No backwall echo was detected in the reference block, which is consistent with the conclusion that the material is equiaxed. No echo signal could be detected on the pump-side elbow, but echoes were present in the generator-side elbow. Thus, the two elbows have distinctly different wave propagation characteristics. However, in both cases there was considerable ultrasonic noise.

These results are consistent with the suppositions that ultrasonic inspections of CSS are very unreliable at best, that ultrasonic-wave propagation characteristics vary considerably from component to component and within an individual component, and that reference-block material may not be representative of the material to be inspected.

2. Microstructure and Deviation of Ultrasonic Beams

In an elastically isotropic material (equiaxed grains), the energy in an ultrasonic beam propagates in the direction of the wavefront normal, as expected. However, in elastically anisotropic material (columnar grain structure), the direction of propagation of ultrasonic energy in a beam can be different from the direction of the wavefront normal. Because of this phenomenon, it may be possible to distinguish columnar from equiaxed grain structures nondestructively by examining the propagation behavior of 45° longitudinal waves in the material. Figure 8 shows the predicted propagation behavior in 60-mm-thick specimens. For an equiaxed specimen with the transmitter and receiver placed on opposite sides (Fig. 8a), the maximum acoustic signal will be detected ∿60 mm from the point directly opposite the beam entry point. For a specimen with columnar grains (Fig. 8b), the energy in the beam deviates markedly from the expected 45° path, such that the maximum signal will be detected at only ∿16 mm from the point opposite the beam entry point. As shown in Fig. 8c, the beam in the equiaxed material will be reflected to a point ∿120 mm from the transmitting transducer (following the expected "full-V" path), while the maximum reflected-beam intensity in the columnar material will be found much closer to the transmitting transducer (∿32 mm away).

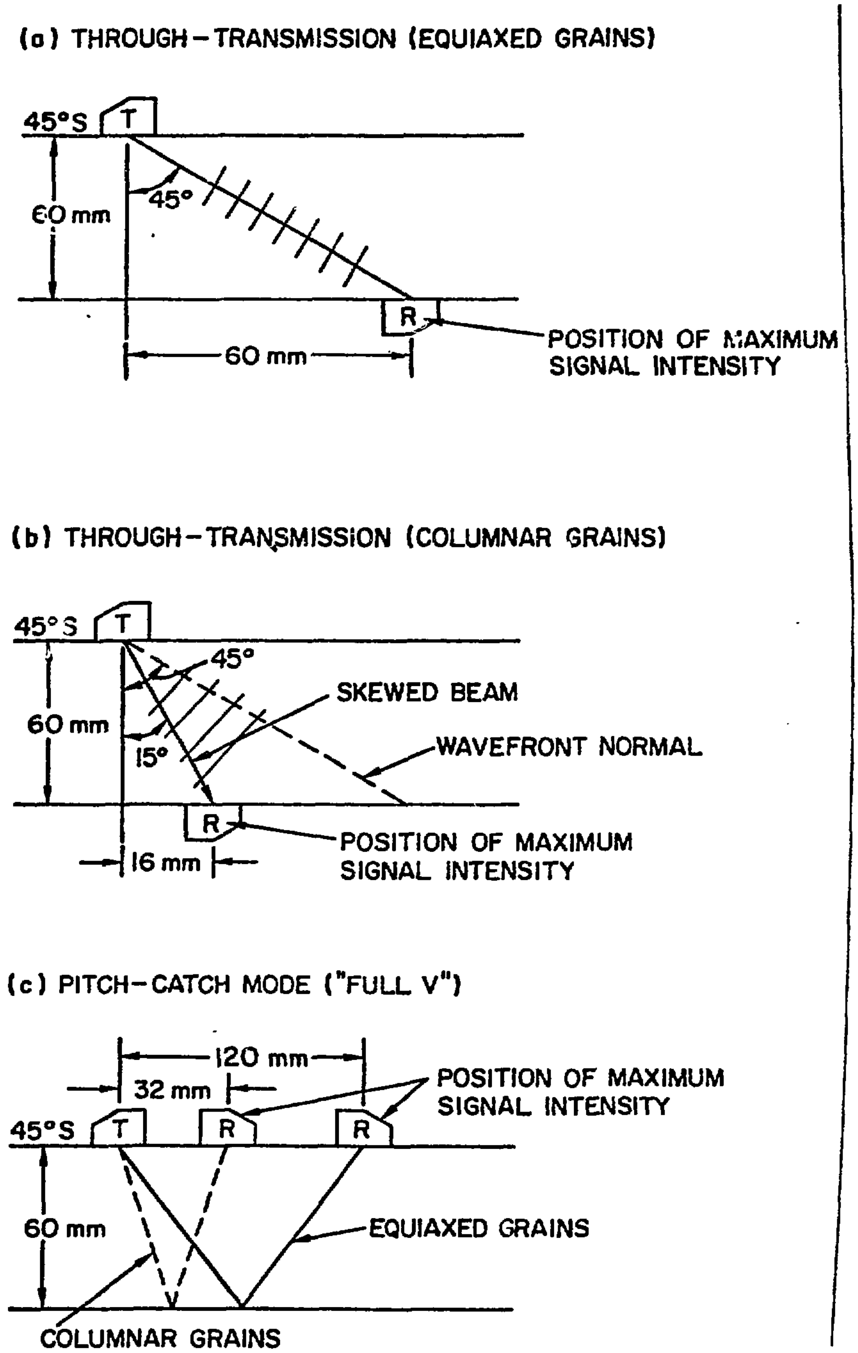

Fig. 8. Schematic Representation of the Path of Ultrasonic Energy in Cast Stainless Steel with Equiaxed and Columnar Grain Structures. (a) Transmit from outer surface and receive at inner (equiaxed grains), (b) transmit from outer surface and receive at inner (columnar grains), and (c) transmit and receive at outer surface.

Experiments were carried out on one columnar and one equiaxed pipe section to verify these predictions. Two 1-MHz, nominally 45° shear-wave transducers (1-in. dia) were placed on the outer surface of each pipe section, and the separation between the two transducers was varied to maximize the received signal. Table 3 compares the optimum separations determined in these experiments with the corresponding predicted values. The agreement is reasonable.

Table 3. Transducer Pair Separation[a] for Maximum Received Signal on Outer Surface of 60-mm-Thick CSS Pipe Sections

Grain Structure	Predicted Value, mm	Measured Value, mm
Columnar	32	42
Equiaxed	127	105

[a] 45° shear waves in pitch-catch "full-V" configuration at 0.5 MHz.

D. Summary

Although the ASME code requires inspection of CSS piping, it has not been possible to demonstrate that current inspection techniques are adequate. For the near term, improvements that may increase the reliability of ultrasonic inspection include (a) the development of methods to establish the microstructure of the material (to help optimize the inspection technique), (b) calibration standards that are more representative of the material to be inspected, and (c) the use of cracked CSS samples for training purposes. For the long term, it will be necessary to establish (a) the variability of the microstructure of CSS, (b) the effect of microstructure on inspection reliability, (c) the degree of improvement possible with techniques and equipment designed specifically for CSS, e.g., focused transducers and lower frequencies than those used conventionally, and (d) qualification of requirements for CSS inspections.